Molecular basis for specific viral RNA recognition and 2′-O-ribose methylation by the dengue virus nonstructural protein 5 (NS5)

Yongqian Zhao[a,b,1], Tingjin Sherryl Soh[c,d,1], Siew Pheng Lim[d], Ka Yan Chung[c,d], Kunchithapadam Swaminathan[b,2], Subhash G. Vasudevan[a,b], Pei-Yong Shi[d,e,f,g,3], Julien Lescar[c,h,i,3], and Dahai Luo[i,j,3]

[a]Program in Emerging Infectious Diseases, Duke-NUS (National University of Singapore) Graduate Medical School, Singapore 169857; [b]NUS Graduate School for Integrative Sciences and Engineering, National University of Singapore, Singapore 117456; [c]School of Biological Sciences, Nanyang Technological University, Singapore 637551; [d]Novartis Institute for Tropical Diseases, Singapore 138670; [e]Department of Biochemistry and Molecular Biology, University of Texas Medical Branch, Galveston, TX 77555-1055; [f]Department of Pharmacology and Toxicology, University of Texas Medical Branch, Galveston, TX 77555-1055; [g]Sealy Center for Structural Biology and Molecular Biophysics, University of Texas Medical Branch, Galveston, TX 77555-1055; [h]Centre d'Immunologie et des Maladies Infectieuses, Centre Hospitalier Universitaire Pitié-Salpêtrière, Faculté de Médecine Pierre et Marie Curie, 75013 Paris, France; [i]Institute of Structural Biology, Nanyang Technological University (NTU), Singapore 636921; and [j]Lee Kong Chian School of Medicine, Nanyang Technological University, Singapore 636921

Edited by Zhijian J. Chen, University of Texas Southwestern Medical Center and Howard Hughes Medical Institute, Dallas, TX, and approved October 27, 2015 (received for review July 29, 2015)

Dengue virus (DENV) causes several hundred million human infections and more than 20,000 deaths annually. Neither an efficacious vaccine conferring immunity against all four circulating serotypes nor specific drugs are currently available to treat this emerging global disease. Capping of the DENV RNA genome is an essential structural modification that protects the RNA from degradation by 5′ exoribonucleases, ensures efficient expression of viral proteins, and allows escape from the host innate immune response. The large flavivirus nonstructural protein 5 (NS5) (105 kDa) has RNA methyltransferase activities at its N-terminal region, which is responsible for capping the virus RNA genome. The methyl transfer reactions are thought to occur sequentially using the strictly conserved flavivirus 5′ RNA sequence as substrate (G_{ppp}AG-RNA), leading to the formation of the 5′ RNA cap: G_{0ppp}AG-RNA→$^{m7}G_{0ppp}$AG-RNA ("cap-0")→$^{m7}G_{0ppp}A_{m2'\text{-}O}$G-RNA ("cap-1"). To elucidate how viral RNA is specifically recognized and methylated, we determined the crystal structure of a ternary complex between the full-length NS5 protein from dengue virus, an octameric cap-0 viral RNA substrate bearing the authentic DENV genomic sequence (5′-$^{m7}G_{0ppp}A_1G_2U_3U_4G_5U_6U_7$-3′), and *S*-adenosyl-L-homocysteine (SAH), the by-product of the methylation reaction. The structure provides for the first time, to our knowledge, a molecular basis for specific adenosine 2′-O-methylation, rationalizes mutagenesis studies targeting the K61-D146-K180-E216 enzymatic tetrad as well as residues lining the RNA binding groove, and offers previously unidentified mechanistic and evolutionary insights into cap-1 formation by NS5, which underlies innate immunity evasion by flaviviruses.

dengue virus | nonstructural protein 5 methyltransferase-polymerase | 2′-O-ribose methyltransferase | cap-0 RNA | innate immunity evasion

Several members of the *Flavivirus* genus from the *Flaviviridae* family are major human pathogens, such as the four serotypes of dengue virus (DENV1–4), West Nile virus (WNV), Japanese encephalitis virus (JEV), and yellow fever virus (YFV). Recent large-scale DENV vaccine trials using a tetravalent formulation and three dose injections have shown only limited protection against the four DENV serotypes, and no specific antiviral drug has reached the market so far (1–3). The flavivirus genome consists of a (+)-sense single-stranded RNA of ∼11 kb with a type 1 cap structure, followed by the strictly conserved dinucleotide sequence "AG": 5′-$^{m7}G_{ppp}A_{m2'\text{-}O}$G-3′ (4, 5). Addition of the cap moiety to the 5′ end of the viral genome is crucial for viral replication, because this structure ensures efficient production of viral polyproteins by the host translation machinery and protection against degradation by 5′-3′ exoribonucleases, and also because it conceals the triphosphorylated (or diphosphorylated) end from recognition by host cell innate immune sensors (6–9). Following (+)-strand RNA synthesis by the C-terminal RNA-dependent RNA polymerase (RdRp) domain of nonstructural protein 5 (NS5), cap formation in flaviviruses results from several sequential enzymatic reactions carried out by (*i*) the RNA triphosphatase activity of the NS3 protease-helicase that hydrolyzes the γ-phosphate group of the viral 5′ untranslated region (UTR), yielding a diphosphate RNA, (*ii*) a guanylyl-transferase activity proposed to reside in the methyltransferase (MTase) domain of NS5, which transfers a GMP molecule to the 5′-diphosphate RNA, and (*iii*) NS5-mediated sequential N-7- and 2′-O-methylations according to the following scheme: G_{0ppp}AG-RNA→$^{m7}G_{0ppp}$AG-RNA ("cap-0")→$^{m7}G_{0ppp}A_{m2'\text{-}O}$G-RNA ("cap-1") (5, 10–12).

During flavivirus RNA replication, 5′-guanosine N-7-methylation is shown to be essential for translation of the viral polyprotein (13), whereas 2′-O-methylation on the penultimate A nucleotide conceals the viral genome from host immune sensors,

Significance

Dengue is the most prevalent mosquito-borne viral disease, endemic in more than a hundred tropical and subtropical countries. NS5, the largest viral protein, is a key replication enzyme with both methyltransferase and RNA polymerase activities. We present to our knowledge the first crystal structure of the full-length NS5 protein from dengue virus bound to the authentic 5′-end viral RNA fragment. This structure captures the viral enzyme in the act of transferring a methyl group to the 2′-O-ribose of the first nucleotide of the viral genome, providing an atomic-level understanding of specific 2′-O-methylation and cap formation by the flavivirus methyltransferase. The structure also suggests an evolutionary origin for the methyltransferase domain of NS5 and strategies for designing novel antiviral inhibitors.

Author contributions: Y.Z., K.S., S.G.V., P.-Y.S., J.L., and D.L. designed research; Y.Z., T.S.S., S.P.L., K.Y.C., J.L., and D.L. performed research; Y.Z., T.S.S., S.P.L., S.G.V., P.-Y.S., J.L., and D.L. analyzed data; and J.L. and D.L. wrote the paper.

The authors declare no conflict of interest.

This article is a PNAS Direct Submission.

Data deposition: The crystallography, atomic coordinates, and structure factors reported in this paper have been deposited in the Protein Data Bank, www.pdb.org (PDB ID code 5DTO).

[1]Y.Z. and T.S.S. contributed equally to this work.

[2]Present address: Department of Biological Sciences, National University of Singapore, Singapore 117543.

[3]To whom correspondence may be addressed. Email: peshi@utmb.edu, julien@ntu.edu.sg, or luodahai@ntu.edu.sg.

This article contains supporting information online at www.pnas.org/lookup/suppl/doi:10.1073/pnas.1514978112/-/DCSupplemental.

notably RIG-I (14), MDA5 (15), and IFIT1 (16–18). Specifically, WNV carrying the E218A mutation in NS5 (E216A in DENV3 NS5) devoid of 2′-O (but not N-7) MTase activity was attenuated in wild-type but not *Ifit1*$^{-/-}$ cells (16). Furthermore, the translation of JEV viral proteins was inhibited by IFIT1 through direct binding to the 5′-capped 2′-O-unmethylated mRNA (17). More recently, 2′-O-methylation at internal adenosines (but not at G, C, or U positions) by the flavivirus NS5 protein was demonstrated. The functional consequence of methylation at internal adenosines was an attenuation of viral RNA translation and replication (12). In vitro, the MTase domain of NS5 catalyzes these two enzymatic reactions with distinct requirements of RNA substrates and buffers: 5′-guanosine N-7 methyl transfer is optimal on a 211-nt segment of the 5′UTR at pH 6 and is inhibited by $MgCl_2$, whereas adenosine ribose 2′-O-methylation only requires a short RNA with "AG" as the first two RNA nucleotides and is maximal at pH 9–10 in the presence of Mg^{2+} ions. Thus, NS5 plays a crucial role both in virus replication and evasion of the host innate immune response, and therefore constitutes an attractive therapeutic target for antiviral drug and vaccine development (2, 19).

Several crystal structures of flavivirus MTases have been reported either as free enzymes or bound to GTP (20), to the broad antiviral nucleoside analog ribavirin (21), to short cap analogs (22, 23), and to a capped-RNA octamer (24). Collectively, these structures uncovered a GTP binding site, the *S*-adenosyl-methionine (SAM) methyl-donor binding pocket, and a basic cleft at the protein surface that was proposed to accommodate the incoming RNA substrate. However, in the absence of a viral RNA in a catalytically meaningful position, the mechanism accounting for specific viral RNA methylation, including the structural basis for specific adenosine 2′-O-methylation, remains elusive. Moreover, the size of the RNA substrate that can be accommodated by the putative RNA binding cleft is also unknown, as well as any requirement for a specific RNA conformation. Determination of the structure of NS5 bound to a viral RNA would give valuable information to guide the design of specific NS5 inhibitors.

To elucidate how the flavivirus RNA is recognized and methylated, we determined the crystal structure of a ternary complex between the full-length NS5 protein (DENV serotype 3), an authentic cap-0 viral RNA substrate (5′-$^{m7}G_{0ppp}A_1G_2U_3U_4G_5U_6U_7$-3′), and *S*-adenosyl-L-homocysteine (SAH), the by-product of the methylation reaction. Together with mutagenesis data informed by the present structure, this work reveals a unique and specific interaction between the protein and viral RNA and provides the molecular basis for the methyl transfer reaction. Furthermore, despite a low sequence identity between the two proteins, the RNA recognition mode is reminiscent of how the human 2′-O-ribose methyltransferase CMTr1 binds mRNA for cap formation, suggesting that the viral methyltransferase might derive from its eukaryotic homolog.

Results and Discussion

Overall Structure of the Ternary Complex of DENV3 NS5, Cap-0 Viral RNA, and SAH. An overall view of bound RNA in the MTase domain of NS5 is given in Fig. 1*A*. The electrostatic surface representation in Fig. 1*B* reveals that the RNA moiety occupies a significant portion of a large basic patch of the NS5 protein. The ordered part of the single-strand RNA substrate consists of the 5′-$^{m7}G_{0ppp}A_1G_2U_3U_4$-3′ sequence (Fig. 1*C*, *SI Appendix*, Fig. S1, and Movie S1). The crystal structure of the ternary complex between NS5, cap-0 RNA, and SAH (Fig. 1) was refined to R_{work} 0.1827, R_{free} 0.2436 at a resolution of 2.6 Å with good stereochemical parameters (Table 1). Bound RNA extends between F25, which is stacked with $^{m7}G_0$ at the 5′ end, and the methyl donor pocket, spanning an overall distance of ∼17 Å across the RNA binding groove. The $^{m7}G_0$ ring makes hydrogen bonds through its N2 atom with the carbonyl oxygen atom of L20 and N18 as well as via its ribose 2′-OH with the N18 side chain (Fig. 1*C*) (13, 20). The N-7-methyl of the $^{m7}G_0$ enhances stacking interactions with F25. The negative charges of the triphosphate group that links $^{m7}G_0$ and A_1 are neutralized by a hexacoordinated Mg^{2+} ion (via three phosphate and three water molecule oxygen atoms, respectively) and hydrogen-bond with residues S213 and S150 that project from the protein surface (Fig. 1*C* and *SI Appendix*, Table S1*A*). The remainder of the RNA ($G_2U_3U_4$) adopts an α-helical conformation along an axis that crisscrosses with the $^{m7}G_{0ppp}$ moiety, giving an overall "L" shape to the bound cap-0 RNA (Fig. 1*C*). The observation of four stacked bases, $A_1G_2U_3U_4$, in addition to $^{m7}G_{0ppp}$ (Fig. 1*C*) is consistent with previous RNase footprinting assays showing that a total of

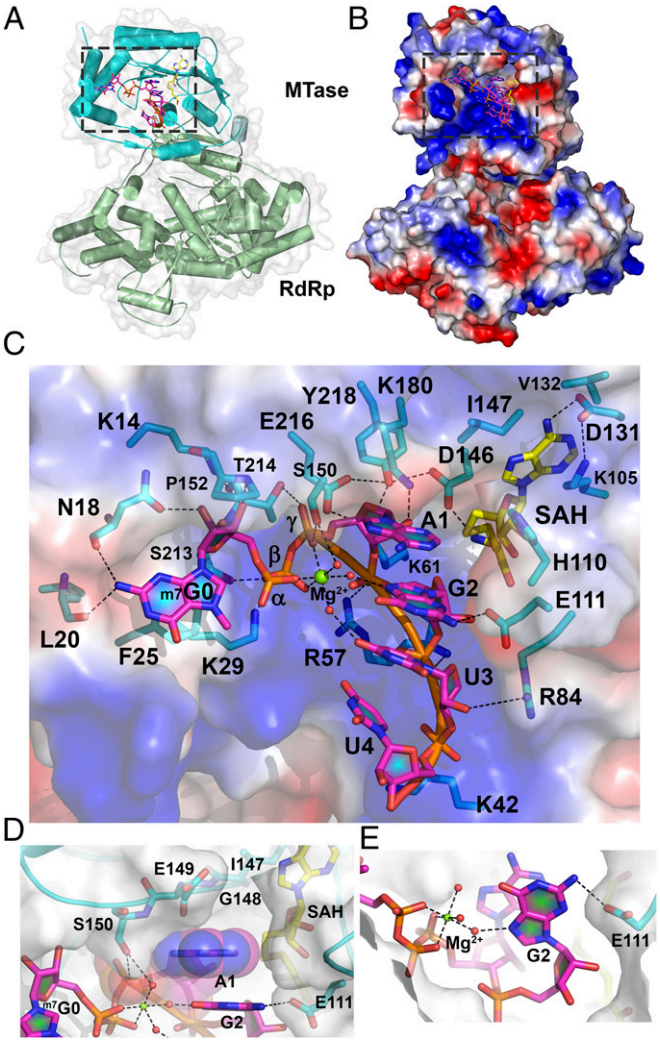

Fig. 1. Structure of the ternary complex between DENV3 NS5, capped RNA, and SAH. (*A*) Crystal structure of NS56–896 (MTase domain, cyan; RdRp domain, green) bound to RNA (5′-$^{m7}G_{0ppp}A_1G_2U_3U_4GUU$-3′; magenta sticks) and SAH (yellow sticks). The RNA/SAH binding site is boxed. (*B*) Electrostatic surface representation of NS5 (positive charges are in blue, and negative charges are in red). Capped RNA (magenta) and SAH (yellow) are shown as sticks. (*C*) Close-up view of the RNA and SAH binding sites as boxed in *B*. Protein residues binding RNA or SAH are represented as sticks (cyan) and labeled. Capped RNA nucleotides are labeled. Dashed lines indicate polar interactions. Mg2+ is displayed as a green sphere, and water molecules are shown as red spheres. (*D*) Interactions established between adenine A1 from the bound RNA and NS5, illustrating the tight shape complementarity with adenine only. (*E*) Hydrogen bonds formed between E111, the capped RNA second nucleotide G2, and the bound Mg2+ ion.

Table 1. Data collection and refinement statistics

Parameters	NS5: Cap-0 RNA: SAH
Data collection statistics	
Resolution range, Å	47.33–2.60 (2.72–2.60)*
Space group	P 2_12_12
Unit cell parameters a, b, c, Å	94.66, 151.39, 69.43
Measured reflections	183,254 (22,200)
Unique reflections	31,327 (3,722)
R_{merge} †	0.175 (1.041)
CC1/2	0.992 (0.641)
Multiplicity	5.8 (6.0)
Completeness, %	99.9 (99.1)
Mean I/sigma(I)	9.9 (1.8)
Refinement statistics	
Resolution range, Å	47.33–2.60 (2.69–2.60)*
R_{work} ‡	0.1827 (0.2857)
R_{free} §	0.2436 (0.3382)
No. of nonhydrogen atoms	7,228
Macromolecules	6,950
Ligands	148
Water	241
Protein residues	852
Rms, bonds, Å	0.003
Rms, angles, °	0.779
Ramachandran plot, %	
Favored	95.04
Allowed	4.6
Outliers	0.35
Clash score	6.53
Average B factor	45.8
Macromolecules	46.0
Ligands	66.6
Solvent	36.1

*The numbers in parentheses refer to the last (highest) resolution shell.
†$R_{merge} = \sum|I_j - < I >|/\sum I_j$, where I_j is the intensity of an individual reflection and $< I >$ is the average intensity of that reflection.
‡$R_{work} = \sum||F_o| - |F_c||/\sum|F_c|$, where F_o denotes the observed structure factor amplitude and F_c denotes the structure factor amplitude calculated from the model.
§R_{free} is as for R_{work} but calculated with 5% (3,044) of randomly chosen reflections omitted from the refinement.

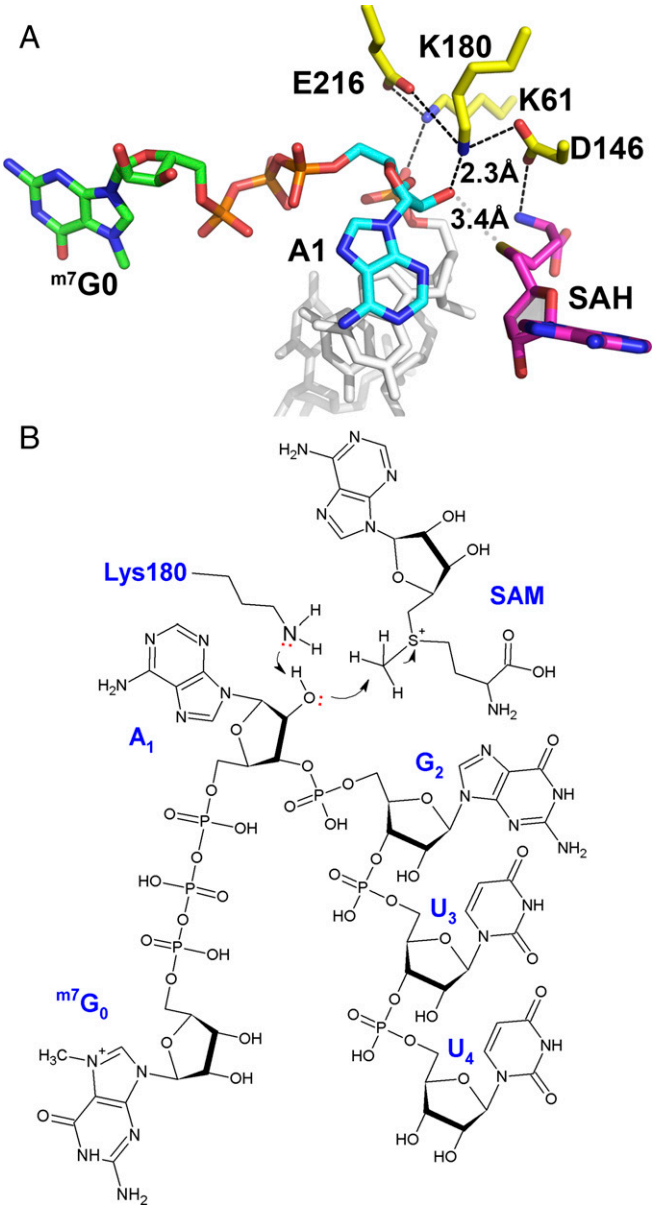

Fig. 2. Proposed enzymatic mechanism for 2′-O-methylation by the flavivirus NS5 MTase. (*A*) Close-up view of the MTase active site with the K_{61}-D_{146}-K_{180}-E_{216} catalytic tetrad shown as yellow sticks and SAH in magenta sticks. Color code for the bound RNA: G_0 carbon atoms, green; A_1, cyan; $G_2U_3U_4$, gray. The close contacts between the 2′-oxygen atom of adenine A_1, the amino group of K_{180}, and the sulfur group of SAH are indicated by dashed lines, and the corresponding distances are given. (*B*) Schematic view of an active ternary complex comprising cap-0 RNA and the methyl donor SAM, based on the present structure. The stereochemistry of the reactants (distances and angles) conforms to what is expected from an inline S_N2 reaction.

4 nt becomes protected by the flavivirus MTase during 2′-O-methylation (13, 25). Only weak electron density is visible for $G_5U_6U_7$ that extends out of the MTase binding groove. In the present conformation, no constraint on the length of the RNA substrate that can be accommodated by the MTase domain seems imposed by the NS5 RdRp domain (Fig. 1 and *SI Appendix*, Fig. S1). To assess possible conformational changes upon substrate binding, we superimposed the present NS5-capped RNA complex with the free NS5 enzyme [Protein Data Bank (PDB) ID code 4V0Q]. This returned an rms value of 0.281 Å for 758 C_α atoms, suggesting an essentially preformed RNA binding groove with no domain reorientation between the MTase and RdRp domains upon binding capped RNA (26). Remarkably, the RNA substrate is positioned such that the 2′-O atom of residue A_1 lies next to the sulfur atom of SAH and adjacent to the K180 side chain from the "K_{61}-D_{146}-K_{180}-E_{216}" enzymatic motif, poised to accept a methyl group from a SAM methyl donor (Figs. 1*C* and 2*A*).

Specificity of Viral RNA Recognition by NS5 MTase. The crystal structure explains the specific recognition of the flavivirus RNA 5′ cap by NS5 and in particular the strict requirement for an adenosine at position 1 and the preference for a guanosine at position 2 (Fig. 1 *D* and *E* and *SI Appendix*, Fig. S2). The first nucleotide of the flavivirus genome, always an adenosine (A_1), resides ∼8 Å away from and nearly perpendicular to $^{m7}G_0$, to which it is connected via the triphosphate 5′–5′ linkage (Fig. 1 *C* and *D*). Remarkably, the A_1 base fits snugly in a pocket shaped by residues I147-G148-E149-S150 from NS5 and SAH (Fig. 1*D*). To understand the origin of specific adenosine 2′-O-methylation by flaviviruses, we modeled X_1 = G, U, or C ($^{m7}G_{0ppp}X_1$-RNA) in place of A_1 and found that the N2 amine group from G_1 would sterically collide with SAH (nearest distance ∼1 Å) (*SI Appendix*, Fig. S2*A*). Conversely, pyrimidine bases would leave a large empty space in the pocket, leading to energetically less favorable van der Waals interactions with the protein (*SI Appendix*, Fig. S2*A*).

Consistently, specific 2′-O-methylations have been identified in viral genomic RNA internal adenosines and polyA but not on polyG, polyC, or polyU substrates (12).

G_2, the second nucleotide of the viral genome, stacks with A_1 and makes a hydrogen bond with the carboxylic side chain of E111 via its N2 atom and with a water molecule coordinating the Mg^{2+} ion (Fig. 1*E* and *SI Appendix*, Fig. S2*B*). We explore below the importance of this polar contact in the context of DENV replication. Modeling X_2 = A, U, or C ($^{7me}G_{0ppp}AX_2$-RNA) in place of G_2 showed that bases other than G disrupt favorable contacts and, in the case of a pyrimidine base, introduces unfavorable charge–charge repulsion between the carboxylic group of E111 and the O2 atom of X_2 = U or C (*SI Appendix*, Fig. S2*B*). Thus, specific recognition of the 5′ end of the flavivirus genome is seen as the consequence of optimum shape complementarity and specific hydrogen bonding between the NS5 protein, the SAM methyl donor, and the 5′ terminus of viral genomic RNA. This observation is consistent with the strict conservation of the 5′ $G_{0ppp}A_1G_2$ sequence during flavivirus genome evolution (*SI Appendix*, Fig. S2*C*) (27). Likewise, residues from the NS5 MTase domain that form the tip of the RNA binding pocket and establish specific polar interactions with the A_1G_2 dinucleotide are also conserved.

Enzymatic Mechanism for Viral RNA 2′-O-Methylation. RNA is bound in the DENV MTase catalytic site, such that the 2′-O-ribose of residue A_1 is placed next to the SAH moiety. This observation suggests that the present complex represents a snapshot along the 2′-O-methylation reaction pathway, possibly the reaction product (Fig. 2 and *SI Appendix*, Fig. S3*A*): (*i*) The side chain of K180 activates the 2′-OH of the adenosine ribose of the RNA methyl acceptor (28), and (*ii*) the activated ribose 2′-O makes a nucleophilic attack on the methyl group of the positively charged sulfur center via an inline S_N2 reaction. At pH 8.5, a value close to the pK_a of the lysine ε-amino-group side chain, where the 2′-O-MTase reaction is maximal (25, 29), the side chain of K180 can be easily deprotonated. Moreover, because K180 is sandwiched between the acidic side chains of D146 and E216, its side chain could alternate between a charged and uncharged species at various stages of the 2′-O-methylation cycle. This scheme is consistent with the available mutagenesis data: The D146A single mutant is completely devoid of 2′-O-methylation activity (*SI Appendix*, Table S1*A*), and its side-chain carboxylic group is at the right distance to stabilize the electrophilic sulfur group of SAM as well as K180, following activation of the 2′-OH adenosine ribose (Fig. 2*A* and *SI Appendix*, Fig. S3) (30). Mutagenesis experiments also indicate that residues F25, R57, and K61 play a major role in the reaction: Alanine mutations at these positions essentially abolish the 2′-O-MTase activity (*SI Appendix*, Table S1*A*). Moreover, the pattern of RNA-enhanced thermostabilization for the DENV MTase is consistent with the observation that amino acids F25, R57, and R61 all make key contacts with RNA in the present complex (29). One attractive hypothesis suggested by the present structure is that the SAM cofactor could act as a "sensor" by probing for the base identity and for the presence of a methyl group(s) in the RNA substrate. Depending on its methylation state, the RNA substrate could either be in a favorable position in the binding groove conducive to methyl transfer or sterically collide with the methyl donor, favoring its dissociation from the MTase domain.

The catalytic mechanism proposed for NS5 is shared with the human mRNA cap-specific 2′-O-ribose methyltransferase CMTr1 and the vaccinia virus VP39 proteins (whose structures with capped RNA are known) and other RNA 2′-O-MTases across all animal kingdoms and viruses whose free enzyme structures have been reported (*SI Appendix*, Fig. S4 and Table S2) (31, 32). However, in contrast to the human CMTr1 or vaccinia virus VP39 that methylates cap-0 RNA substrates in a sequence-independent manner, the flavivirus NS5 MTase has a demonstrated RNA substrate sequence specificity, which is evident in our structure analysis and functional studies (Figs. 1, 3, and 4). A requirement for Mg^{2+} ions was reported for the COMT MTase as well as for FtsJ 2′-O-methylation activities (33, 34), and Mg^{2+} has stimulatory effects on DENV 2′-O-MTase activity (35). The structure of COMT suggested that Mg^{2+} ions play an important role for RNA stabilization but not for catalysis. Given the close similarity between the active sites of VP39 and FtsJ, Mg^{2+} ions are thought to be dispensable for 2′-O-methylation (34). Thus, activity enhancement in the presence of Mg^{2+} in DENV NS5 appears to be due to structural and electrostatic stabilization of the protein–RNA complex.

Flavivirus NS5 MTase Is Closest to the Human mRNA Cap-Specific 2′-O-Ribose CMTr1. To gain insights into the evolution leading to the present NS5 MTase domain, we performed a homology search against the various available MTase structures (36). The

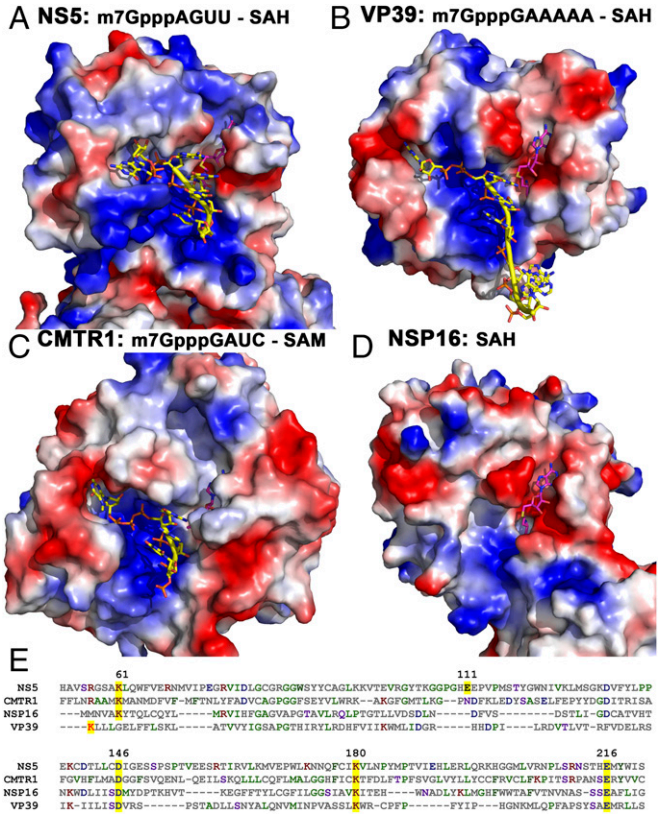

Fig. 3. Comparison of NS5 MTase with other human and viral 2′-O-MTases. (*A*) The DENV3 NS5 MTase (this work). (*B*) Vaccinia virus MTase VP39. (*C*) Human CMTr1. (*D*) Severe acute respiratory syndrome (SARS) coronavirus MTase nonstructural protein 16 (NSP16). The comparison highlights the variety of shape complementarity and surface charge distributions between the enzymes, cofactor, and RNA substrate. The VP39 G_0 pocket is deeper and more distant from the RNA binding groove compared with NS5 and CMTr1. As a result, G_0 is deeply buried, with a protruding ribose. In contrast, no apparent G_0 binding pocket is found in NSP16. Triphosphates display various conformations: extended in VP39 and CMTr1, and bent in NS5. In all three complexes, four RNA bases occupy the positively charged groove. The RNA binding groove in nsp16 is shallow and less positively charged. The SAM binding pocket is the most conserved feature, except at the adenine binding site: In NS5, a positively charged pocket is located next to N-7, whereas in CMTr1, the corresponding pocket is deeper and larger; in VP39, it is open and negatively charged. In nsp16, no apparent pocket is visible. Positive protein surfaces are shown in blue, and negative surfaces are in red; RNA moieties (yellow carbons) and SAH/SAM (magenta carbons) are shown as sticks. (*E*) Multiple sequence alignment. The K-D-K-E catalytic tetrad is highlighted in yellow. E111 from DENV NS5 is also highlighted.

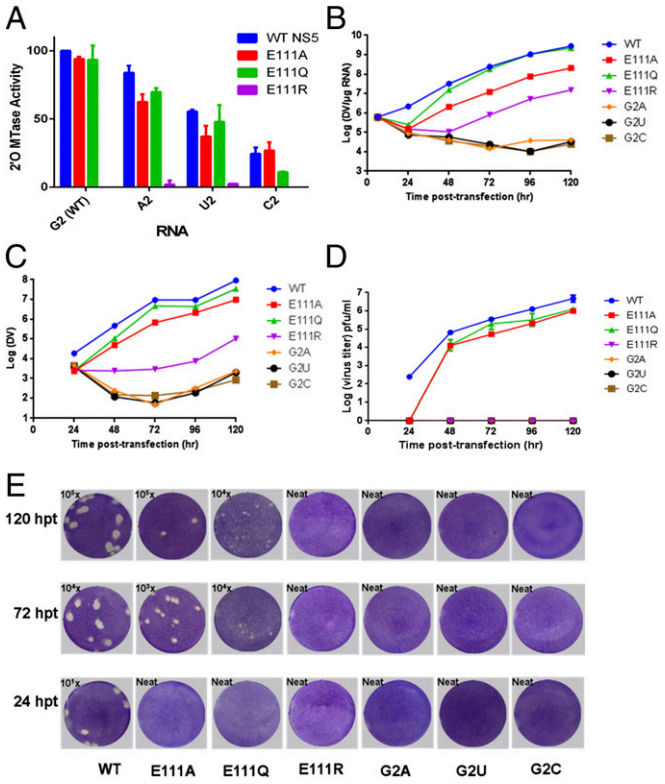

Fig. 4. Specific recognition of the capped viral RNA is essential for virus replication. (*A*) In vitro 2′-O-MTase activities of WT NS5 and E111 mutants using WT and mutant RNA templates. Data are normalized to the activity of the WT NS5 MTase on WT viral 5′UTR RNA, which is set to 100% (corresponding to ∼4 nM ^{3}H-methyl incorporated into the RNA; signal-to-background count ratios are approximately four- to fivefold). Each data point is the average for three replicates, and error bars show the standard deviations. (*B*) Intracellular viral RNA levels detected by quantitative (q)RT-PCR. (*C*) Extracellular viral RNA levels in the supernatants detected by qRT-PCR. (*D*) Virus titers based on the plaque assay shown in *E*. (*E*) Plaque assay for WT and mutants at 24, 72, and 120 h posttransfection (hpt). The limits of detection for DENV genomic RNA by qRT-PCR and plaque assays are 100 copies and 1 infectious virus particle, respectively.

flavivirus NS5 protein belongs to a family of SAM-dependent RNA MTases that methylate diverse RNA species including mRNA, rRNA, tRNA, and siRNA, either at the bases or at 2′-hydroxyl groups of specific nucleosides. Within the *Flavivirus* genus, both the primary sequence and the 3D structures of the MTase domain are highly conserved, with sequence identities ranging from 51% to 100% (*Z* scores of 32.2–43.8). Surprisingly, despite a low sequence identity of 14% between the two proteins, the closest NS5 structural homolog with an rmsd of 2.9 Å for 222 of the 406 CMTr1 α-carbon atoms and a *Z* score of 15.8 is the human mRNA cap-specific 2′-O-ribose MTase CMTr1 (PDB ID code 4N48). Moreover, the seven next-closest homologs are also of nonviral origin (Fig. 3 and *SI Appendix*, Fig. S4 and Table S2). These structures share the general αβα-Rossmann-fold core domain that shapes the SAM binding pocket and the highly conserved K-D-K-E catalysis tetrad, which is consistent with a common catalytic mechanism for methyl transfer. Structural divergence beyond the core domain likely reflects the present variety of RNA substrate preferences (e.g., 2′-O-ribose of capped RNA vs. ribosomal RNA methylation) (37, 38). Thus, the flavivirus NS5 MTase domain might derive from its eukaryotic homolog. Interestingly, the *Flavivirus* genus is the only clade in the *Flaviviridae* family that encodes an MTase at the N terminus of NS5. Considering that the RdRp domain is highly conserved in all viruses from the *Flaviviridae* family but is absent from the host cells, the present flavivirus NS5 protein might have originated from a domain fusion event through the acquisition of an RNA 2′-O-MTase domain from the host following the separation from the Hepatitis, Pestivirus, and Pegivirus of the *Flaviviridae* family (26).

Residue E111 Is Key for Virus Replication. To investigate the functional implications of the present ternary complex for virus replication, we performed a mutagenesis study targeting the highly conserved residue E111 of NS5, which establishes the sole direct specific polar contact with the second base (G_2) of the flavivirus RNA (Figs. 1*C* and 4 and *SI Appendix*, Fig. S2*B*). We evaluated the effects of E111 mutants both in vitro, using an NS5 MTase enzymatic assay (Fig. 4*A* and *SI Appendix*, Table S1*B*), and also in cell culture by examining the growth kinetics of the corresponding virus mutants (Fig. 4 *B*–*E*). Reversing the charge through the E111R mutation abolishes 2′-O-MTase activity (Fig. 4*A*). In contrast, mutants E111A and E111Q retain >93% activity, which is consistent with a limited impact of these mutations on protein–RNA interaction (Fig. 4*A* and *SI Appendix*, Table S1*B*). Modeling the E111A and E111Q mutations in the NS5–cap-0 RNA suggests that these two mutations have a smaller impact on the ability of the protein to bind cap-0 viral RNA compared with the E111R mutation, which is likely to introduce steric hindrance with the RNA moiety (*SI Appendix*, Fig. S2*D*). These modeling results are in line with experimental thermostability measurements of the corresponding NS5 wild-type and mutant proteins in their free states and in the presence of cap-0 RNA: The E111R mutant has the most decreased thermostability both in the presence and absence of the RNA ligand (*SI Appendix*, Table S1*C*).

Substituting $X_2 = U_2$ or C_2 in place of G_2 ($^{7me}G_{0ppp}AX_2$-RNA) introduces unfavorable electrostatic contacts between their O2 atom and the carboxylic group of E111 and, for $X_2 = A_2$, between N3 and E111 (*SI Appendix*, Fig. S2*B*). This is consistent with the observation that the consensus sequence $G_{0ppp}A_1G_2X$ found in flaviviruses (*SI Appendix*, Fig. S2*C*) binds more tightly than $G_{0ppp}A_1C_2X$ to the DENV MTase (23). Moreover, mutations of G_2 to U, C, or A reduce the 2′-O-methylation activity of NS5 down to 33%, 19%, and 100%, respectively, in WNV (31) and to 55%, 24%, and 84% in DENV4 (*SI Appendix*, Table S1*B*). The corresponding DENV mutants G2A, G2U, and G2C completely fail to grow (Fig. 4 *B*–*E*), showing that the virus does not tolerate changes at position G_2. Because these substitutions preserve 2′-O-MTase activity appreciably, their impact on virus growth is likely to derive at least in part from a different process, possibly the de novo initiation of polymerization by NS5, where a strict requirement for $pppA_1G_2$ was demonstrated (39).

We also found that E111 plays a crucial role in viral replication (Fig. 4 *B*–*E*). The E111Q and E111A mutations attenuated virus replication and produced three to four times less infectious virus, whereas the E111R mutation severely impaired viral replication and yielded no virus (Fig. 4*E*). Mutants such as WNV-E218A abolishing 2′-O-MTase activity yet growing to relatively wild-type levels in BHK or Vero cells have been described (16). Therefore, the origin of the strong attenuation observed for the E111R mutant virus might be multifactorial: E111R is less thermostable than WT protein (*SI Appendix*, Table S1*B*) and has lower elongation polymerase activity, probably due to its poorer ability to bind RNA (*SI Appendix*, Table S1*C*). Together, these effects are likely to cause the mutant virus to be highly attenuated.

Concluding Remarks

The structure presented here suggests possible routes for the design of inhibitors targeting the NS5 MTase catalytic site. One possible strategy would consist of extending SAM analogs toward the RNA binding groove, for instance by linking the A_1 moiety to nucleoside analogs (e.g., ribavirin) that bind at the GTP binding

site, next to residue F25. This strategy may lead to larger but more specific and potent flavivirus MTase inhibitors (40). Also, the effect of MTase mutant on polymerase activities suggests the interdependence of two domains in viral replication (41). Our study also indicates that attenuated viruses could be designed by targeting the E111 residue of NS5.

Materials and Methods

Methods used in this study are briefly summarized below. Full descriptions are given in *SI Appendix, Materials and Methods*.

Protein Expression and Purification. The protocol for NS5 protein expression and purification was as previously described (26).

Crystallization and Data Collection. Crystallization was set up at 20 °C using the hanging-drop vapor-diffusion method and published conditions (26). Native crystals obtained over 2–5 d by mixing a volume of 1 μL NS5 (residues 6–895) at 4–6 mg/mL with 1 μL precipitation solution [0.2 M magnesium acetate, 0.1 M sodium cacodylate, pH 6.4, 10–20% (wt/vol) PEG 8000] were soaked with 1 mM 5′-$^{7me}G_{0ppp}A_1G_2U_3U_4G_5U_6U_7$-3′ overnight.

Structure Solution and Refinement. The crystal had a Matthews coefficient (V_m) of 2.47 (42). Refinement was initiated with the structure PDB ID code 4V0Q using REFMAC5 (43) and PHENIX (44) and interspersed with manual model-rebuilding sessions using Coot (45). The refined coordinates were deposited in the PDB under ID code 5DTO.

Construction of Mutant ^{m7}Gppp-DENV4 5′UTR Nt-110 RNAs for 2′-O-MTase Assay. DENV4 5′UTR nt-110 DNA with substitutions at the position of the 5′ nucleotide G_2 was engineered by PCR using Phusion DNA Polymerase with standard procedures.

DENV4 2′-O-MTase Assay. DENV4 2′-O-MTase assay was performed as described previously (11, 35).

Construction of Mutant DENV2 Full-Length Infectious Clone. DENV2 full-length cDNA clones with NS5 E111A, E111Q, and E111R mutations were constructed with a pACYC-NGC FL and a TA-NGC (shuttle E) vector as previously described (46).

ACKNOWLEDGMENTS. We thank Drs. Liew Chong Wai and Chen Ming Wei and scientists from Swiss Light Source beamline PXIII and Taiwan Republic of China National Synchrotron Radiation Research Centre beamline ID13 for their help with diffraction data collection. We thank Dr. George Chandy for critically reading our manuscript and Dr. Gérard Bricogne (Global Phasing) for advice on refinement with Buster. This work was supported by (*i*) a start-up grant to the D.L. laboratory from Lee Kong Chian School of Medicine, Nanyang Technological University, (*ii*) National Medical Research Council Grant CBRG14May051 (to J.L.), (*iii*) an MOE Tier 1 Complexity grant (to the J.L. laboratory), and (*iv*) National Medical Research Council Grant NMRC/1315/2011 (to the S.G.V. laboratory). Y.Z. is supported by a National University of Singapore Graduate School for Integrative Sciences and Engineering (NGS) scholarship, and T.S.S. is supported by an Industrial Postgraduate Programme Scholarship from the Economic Development Board, Singapore.

1. Capeding MR, et al.; CYD14 Study Group (2014) Clinical efficacy and safety of a novel tetravalent dengue vaccine in healthy children in Asia: A phase 3, randomised, observer-masked, placebo-controlled trial. *Lancet* 384(9951):1358–1365.
2. Lim SP, et al. (2013) Ten years of dengue drug discovery: Progress and prospects. *Antiviral Res* 100(2):500–519.
3. Low JG, et al. (2014) Efficacy and safety of celgosivir in patients with dengue fever (CELADEN): A phase 1b, randomised, double-blind, placebo-controlled, proof-of-concept trial. *Lancet Infect Dis* 14(8):706–715.
4. Lindenbach BD, Thiel HJ, Rice CM (2007) *Flaviviridae: The Viruses and Their Replication* (Lippincott-Raven, Philadelphia).
5. Decroly E, Ferron F, Lescar J, Canard B (2012) Conventional and unconventional mechanisms for capping viral mRNA. *Nat Rev Microbiol* 10(1):51–65.
6. Pichlmair A, et al. (2006) RIG-I-mediated antiviral responses to single-stranded RNA bearing 5′-phosphates. *Science* 314(5801):997–1001.
7. Hornung V, et al. (2006) 5′-Triphosphate RNA is the ligand for RIG-I. *Science* 314(5801):994–997.
8. Rehwinkel J, et al. (2010) RIG-I detects viral genomic RNA during negative-strand RNA virus infection. *Cell* 140(3):397–408.
9. Goubau D, et al. (2014) Antiviral immunity via RIG-I-mediated recognition of RNA bearing 5′-diphosphates. *Nature* 514(7522):372–375.
10. Ray D, et al. (2006) West Nile virus 5′-cap structure is formed by sequential guanine N-7 and ribose 2′-O methylations by nonstructural protein 5. *J Virol* 80(17):8362–8370.
11. Chung KY, et al. (2010) Higher catalytic efficiency of N-7-methylation is responsible for processive N-7 and 2′-O methyltransferase activity in dengue virus. *Virology* 402(1):52–60.
12. Dong H, et al. (2012) 2′-O methylation of internal adenosine by flavivirus NS5 methyltransferase. *PLoS Pathog* 8(4):e1002642.
13. Dong H, et al. (2014) Flavivirus RNA methylation. *J Gen Virol* 95(Pt 4):763–778.
14. Schuberth-Wagner C, et al. (2015) A conserved histidine in the RNA sensor RIG-I controls immune tolerance to N1-2′O-methylated self RNA. *Immunity* 43(1):41–51.
15. Züst R, et al. (2011) Ribose 2′-O-methylation provides a molecular signature for the distinction of self and non-self mRNA dependent on the RNA sensor Mda5. *Nat Immunol* 12(2):137–143.
16. Daffis S, et al. (2010) 2′-O methylation of the viral mRNA cap evades host restriction by IFIT family members. *Nature* 468(7322):452–456.
17. Kimura T, et al. (2013) Ifit1 inhibits Japanese encephalitis virus replication through binding to 5′ capped 2′-O unmethylated RNA. *J Virol* 87(18):9997–10003.
18. Habjan M, et al. (2013) Sequestration by IFIT1 impairs translation of 2′O-unmethylated capped RNA. *PLoS Pathog* 9(10):e1003663.
19. Li SH, et al. (2013) Rational design of a flavivirus vaccine by abolishing viral RNA 2′-O methylation. *J Virol* 87(10):5812–5819.
20. Egloff MP, Benarroch D, Selisko B, Romette JL, Canard B (2002) An RNA cap (nucleoside-2′-O-)-methyltransferase in the flavivirus RNA polymerase NS5: Crystal structure and functional characterization. *EMBO J* 21(11):2757–2768.
21. Benarroch D, et al. (2004) A structural basis for the inhibition of the NS5 dengue virus mRNA 2′-O-methyltransferase domain by ribavirin 5′-triphosphate. *J Biol Chem* 279(34):35638–35643.
22. Bollati M, et al. (2009) Recognition of RNA cap in the Wesselsbron virus NS5 methyltransferase domain: Implications for RNA-capping mechanisms in *Flavivirus*. *J Mol Biol* 385(1):140–152.
23. Egloff MP, et al. (2007) Structural and functional analysis of methylation and 5′-RNA sequence requirements of short capped RNAs by the methyltransferase domain of dengue virus NS5. *J Mol Biol* 372(3):723–736.
24. Yap LJ, et al. (2010) Crystal structure of the dengue virus methyltransferase bound to a 5′-capped octameric RNA. *PLoS One* 5(9):e12836.
25. Zhou Y, et al. (2007) Structure and function of flavivirus NS5 methyltransferase. *J Virol* 81(8):3891–3903.
26. Zhao Y, et al. (2015) A crystal structure of the dengue virus NS5 protein reveals a novel inter-domain interface essential for protein flexibility and virus replication. *PLoS Pathog* 11(3):e1004682.
27. Paranjape SM, Harris E (2009) in *Control of Dengue Virus Translation and Replication, Current Topics in Microbiology and Immunology*, Vol 338, ed Rothman AL (Springer, Berlin), pp 15–34.
28. Li C, Xia Y, Gao X, Gershon PD (2004) Mechanism of RNA 2′-O-methylation: Evidence that the catalytic lysine acts to steer rather than deprotonate the target nucleophile. *Biochemistry* 43(19):5680–5687.
29. Dong H, et al. (2010) Biochemical and genetic characterization of dengue virus methyltransferase. *Virology* 405(2):568–578.
30. Dong H, et al. (2008) West Nile virus methyltransferase catalyzes two methylations of the viral RNA cap through a substrate-repositioning mechanism. *J Virol* 82(9):4295–4307.
31. Smietanski M, et al. (2014) Structural analysis of human 2′-O-ribose methyltransferases involved in mRNA cap structure formation. *Nat Commun* 5:3004.
32. Hodel AE, Gershon PD, Quiocho FA (1998) Structural basis for sequence-nonspecific recognition of 5′-capped mRNA by a cap-modifying enzyme. *Mol Cell* 1(3):443–447.
33. Vidgren J, Svensson LA, Liljas A (1994) Crystal structure of catechol O-methyltransferase. *Nature* 368(6469):354–358.
34. Hager J, Staker BL, Bügl H, Jakob U (2002) Active site in RrmJ, a heat shock-induced methyltransferase. *J Biol Chem* 277(44):41978–41986.
35. Lim SP, et al. (2008) A scintillation proximity assay for dengue virus NS5 2′-O-methyltransferase—Kinetic and inhibition analyses. *Antiviral Res* 80(3):360–369.
36. Holm L, Rosenstrom P (2010) Dali server: Conservation mapping in 3D. *Nucleic Acids Res* 38(Web Server issue):W545–W549.
37. Ghosh A, Lima CD (2010) Enzymology of RNA cap synthesis. *Wiley Interdiscip Rev RNA* 1(1):152–172.
38. Wang SP, Deng L, Ho CK, Shuman S (1997) Phylogeny of mRNA capping enzymes. *Proc Natl Acad Sci USA* 94(18):9573–9578.
39. Selisko B, et al. (2012) Molecular basis for nucleotide conservation at the ends of the dengue virus genome. *PLoS Pathog* 8(9):e1002912.
40. Lim SP, et al. (2011) Small molecule inhibitors that selectively block dengue virus methyltransferase. *J Biol Chem* 286(8):6233–6240.
41. Zhao Y, et al. (2015) Flexibility of NS5 methyltransferase-polymerase linker region is essential for dengue virus replication. *J Virol* 89(20):10717–10721.
42. Matthews BW (1968) Solvent content of protein crystals. *J Mol Biol* 33(2):491–497.
43. Collaborative Computational Project, Number 4 (1994) The CCP4 suite: Programs for protein crystallography. *Acta Crystallogr D Biol Crystallogr* 50(Pt 5):760–763.
44. Adams PD, et al. (2010) PHENIX: A comprehensive Python-based system for macromolecular structure solution. *Acta Crystallogr D Biol Crystallogr* 66(Pt 2):213–221.
45. Emsley P, Cowtan K (2004) Coot: Model-building tools for molecular graphics. *Acta Crystallogr D Biol Crystallogr* 60(Pt 12 Pt 1):2126–2132.
46. Xie X, Gayen S, Kang C, Yuan Z, Shi PY (2013) Membrane topology and function of dengue virus NS2A protein. *J Virol* 87(8):4609–4622.